J. Membrane Biol. 133, 1–15 (1993)

The Journal of
Membrane
Biology

Characterization and Cyclic AMP-Dependence of a Hyperpolarization-Activated Chloride Conductance in Leydig Cells from Mature Rat Testis

Jean-François Noulin and Michel Joffre
Laboratoire de Physiologie Animale-URA CNRS 290 Biomembranes, UFR Sciences, 86022-Poitiers, France

Summary. We recently described a cyclic AMP-activated current in the membrane of Leydig cells from mature rat testis by using the whole-cell configuration of the patch-clamp technique (Noulin & Joffre, 1992*a*). In the present study, further experiments were performed in symmetrical CsCl solutions. We show that this current corresponds to a hyperpolarization-activated chloride conductance. Voltage jumps to negative potentials, applied from a holding potential of +60 mV, activated a time-dependent inward current.

In control cells, the curve of steady-state current activation typically ranged from +60 mV (0) to −120 mV (1) and had its midpoint at −40 mV. Deactivation at positive potential was characterized by an instantaneous outwardly rectifying current which decayed with time. The kinetics of activation and deactivation were described by a double and a single exponential, respectively.

Cyclic AMP, added to the pipette solution, increased both the inward rectification and the amplitude of the steady-state current in the range of 0 to −60 mV. The activation threshold was unchanged, while the $V_{0.5}$ of the activation curve was shifted by 24 mV to more positive potentials. Consequently, the activation curve was steeper. The two rate constants of activation were increased and were strongly voltage dependent. In parallel, the amplitude of the instantaneous outward current and the rate constant of deactivation were increased.

The reversal potential of this current was close to E_{Cl}. It did not change with equimolar replacement of cesium by TEA, and shifted with the chloride concentration gradient. This current was inhibited by chloride channel blockers.

These results indicate a hyperpolarization-activated chloride conductance in the membrane of Leydig cells which is modulated by cyclic AMP. This nucleotide acts by modifying the kinetics of inward current and both the kinetics and the amplitude of deactivating outward current.

Key Words hyperpolarization-activated · chloride · conductance · membrane current · Leydig cells · cyclic-AMP dependence

Introduction

The Leydig cells that secrete testosterone in mammalian testes possess receptors for luteinizing hormone (LH). Numerous biochemical studies have contributed to elucidate the intracellular mechanisms involved in the stimulation by this pituitary gonadotropin: high LH or hCG (human Chorionic Gonadotropin) concentrations stimulate the Leydig cell steroidogenesis via a cyclic AMP-kinase A pathway (for review, *see* Dufau, 1988).

As the patch-clamp method has largely contributed to clarify some cellular mechanisms of the action of messengers, we have used it to investigate the control of Leydig cells by LH or hCG. In unstimulated cells, the predominant ionic conductance is a voltage-dependent potassium conductance resembling the delayed rectifier potassium conductance of T-lymphocytes (Duchatelle & Joffre, 1987, 1990).

Two different chloride currents are induced by depolarizations, applied to cells dialyzed with calcium and cyclic AMP (Duchatelle & Joffre, 1987, 1990; Noulin & Joffre, 1992*a*). Both are sensitive to an E_{Cl} displacement and are affected by 1 mM SITS or DIDS, two stilbene-derived chloride channel blockers (Noulin & Joffre, 1992*a*). In the presence of internal calcium, current traces showed the well-known "on" and "off" relaxations characteristic of the calcium-dependent chloride conductance. This conductance increases when the membrane voltage is stepped and thus gives rise to a current increase. By contrast, in the presence of cyclic AMP, voltage jumps to +60 mV or above induced outward currents peaking instantaneously and then inactivating progressively (Noulin & Joffre, 1992*a*). These relaxations are also recorded when cells are dialyzed with GTP or stimulated by LH and hCG (Duchatelle & Joffre, 1990).

At the holding potential of −40 mV (close to the resting membrane potential), the cyclic AMP-dependent chloride conductance, but not the calcium-dependent conductance, is activated. This leads us to record an inward holding current when cells are bathed in symmetrical chloride concentrations. In the present study, we examine more precisely

the properties of this current in symmetrical cesium chloride solutions. We show that this current corresponds to a hyperpolarization-activated chloride conductance, which is slowly activated by long hyperpolarizing pulses and rapidly deactivated by large depolarizations. This conductance corresponds to a small conductance, sensitive to cyclic AMP, in resting cells. Preliminary accounts of this work have been published in abstract form (Noulin & Joffre, 1992*b*).

Materials and Methods

Leydig Cell Preparation

Leydig cells were dispersed from the testes of mature rats as previously described (Duchatelle & Joffre, 1990). Briefly, the testes were removed from 60- to 90-day-old rats and incubated in a solution containing 0.5 mg/ml collagenase (Serva, 0.6–0.8 U/mg) and 0.04 mg/ml trypsin inhibitor (Sigma, St. Louis, MO, soybean-type 1S). The dispersed cells were isolated by density centrifugation on Percoll®. Cells were cultured during a period ranging from 4 hr to 2 day, on 35-mm plastic petri dishes in RPMI 1640 medium (GIBCO, UK) supplemented as indicated by Sharpe and Cooper (1987).

Electrophysiology

Current recordings were obtained using the whole-cell configuration of the patch-clamp technique as described by Marty and Neher (1983), with a patch-clamp amplifier (EPC-7, List Medical, Darmstadt, Germany). Recording pipettes were formed from borosilicate glass capillary tubing (GC 150-TF 10, Clark Electromedical Instruments, UK). They were coated with Sylgard 184 (Dow Corning, Seneffe, Belgium) and fire-polished. Their resistance ranged from 1 to 3 MΩ. The pipette solution was connected to the head stage of an amplifier through a Ag/AgCl pellet. Seal resistances ranged from 3 to 15 GΩ.

The voltage-clamp programs and data collection were performed with an IBM microcomputer (PC AT 286) equipped with a A/D-D/A conversion board (TM-40, Teckmar) and a specific software (pCLAMP 5.5.1, Axon Instruments). Cell currents were low-pass filtered at 3.3 kHz. They were then digitized on-line at 4 kHz and stored on disc. Instantaneous current amplitudes were measured 7 msec after applying a voltage step. They were analyzed off-line with the pCLAMP software after being filtered (cut-off frequency: 0.3 kHz). Electrode capacitance was compensated electronically in cell-attached mode. Membrane capacitance and series resistance were measured in the whole-cell mode by fitting a capacitance record with a first-order exponential and by integrating the surface of capacitance peaks. They were not compensated. Average series resistance and membrane capacitance for 63 cells were respectively 7.7 ± 0.5 MΩ and 22.5 ± 1.0 pF. Because large currents were measured, the test potentials given in the legends of figures were corrected for voltage drop across the series resistances. Liquid junction potentials were canceled before seal formation. To determine time constants for activation and deactivation, current traces were fitted with exponentials using Clampfit software (pCLAMP 5.5.1). Current traces illustrating representative records, current-voltage curves and other data were drawn with a specific software (Fig.P 6, Biosoft, UK).

Solutions

At the beginning of each experiment, the petri dish was rinsed four times with the standard external solution to remove the remaining germinal cells. This solution consisted of (mM): 146 CsCl, 2 $CaCl_2$, 10 HEPES/CsOH, buffer pH 7.4. After rupturing the membrane, the cell was bathed in a stream of calcium-free control medium which flowed out of a capillary with an internal diameter of 250 μm. This solution consisted of (mM): 150 CsCl, 10 HEPES/CsOH buffer, pH 7.4. To investigate the ionic nature of the currents, CsCl was equimolarly replaced by 150 mM TEA (tetraethylammonium) chloride or by 130 mM Cs-glutamate. In the latter case, current voltage curves were corrected for liquid junction potentials. The pipette contained (mM): 144 CsCl, 2.9 $MgCl_2$, 3 ATP-MG, 5 EGTA, 10 HEPES/CsOH buffer, pH 7.2.

Two methods were used to study the dependence of currents on internal cyclic AMP. (i) We compared results from different cells dialyzed either with ATP alone (control cells) or with ATP and 0.1 mM cyclic AMP. To estimate cell-to-cell variations, the experimental values are given as means ± SEM, for n values. The statistical significance of the results was assessed by means of a Student's t-test for unpaired data. (ii) In the second method, we used a cyclic AMP analogue (8-[4-chlorophenylthio]cyclic AMP, PSCl cyclic AMP), which penetrates easily into intact cells.

All experiments were performed at room temperature (20–23 °C).

Chemicals

Glutamic acid, HEPES (N-[2-hydroxyethyl]-N′-[2-ethanesulfonic] acid), 9-AC (anthracene-9-carboxylic acid), cyclic AMP (cyclic adenosine 3′ 5′ monophosphate-sodium salt), DIDS (4, 4′-diisothiocyanatostilbene-2,2′-disulfonic acid) TEA (tetraethylammonium chloride), EGTA (ethylene glycol-bis[β-amino ethyl ether] N,N,N′,N′-tetraacetic acid), ATP-Mg salt; (adenosine triphosphate magnesium salt) were purchased from Sigma (St. Louis, MO); DMSO (dimethylsulfoxide) from Merck (Darmstadt, Germany); PSCl-cyclic AMP (8-[4-chlorophenylthio]cyclic AMP) from Boeringher-Mannheim (Germany). DPC (diphenylamine-2-carboxylic acid) from Fluka (Buchs, Switzerland); cesium chloride and cesium hydroxyde from Aldrich (Strasbourg, France). All these drugs were directly dissolved in the solutions except for 9-AC and DPC which were dissolved in DMSO as 50 mM stock solutions (Singh et al., 1991) and then added to the external medium at the final concentration of 1 mM. Currents in control experiments were not altered by DMSO (2%).

Results

Voltage-Clamp Experiments at a Negative Holding Potential

This study was first performed on Leydig cells bathed in symmetrical CsCl solutions containing ATP-Mg salt. Short voltage steps were applied from

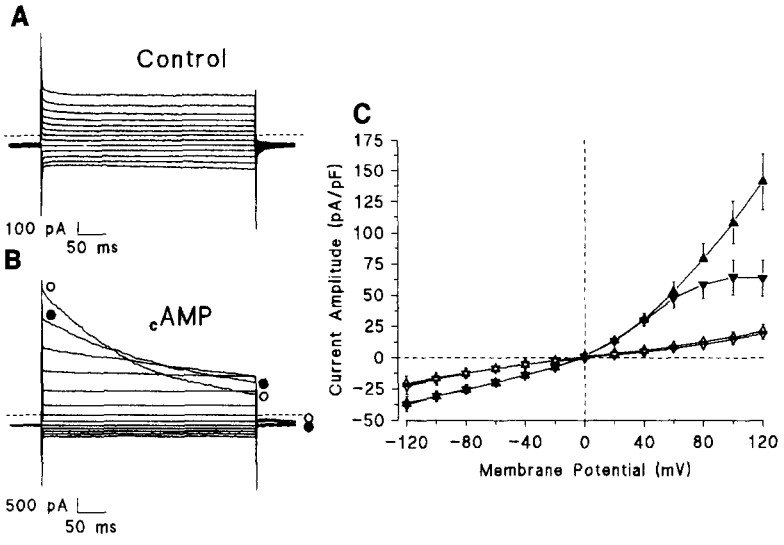

Fig. 1. Whole-cell currents from cells under control conditions (*A*) and in the presence of cyclic AMP (*B*). Pulses (375 msec) were applied every 10 sec from −40 mV to potentials varying from −120 to +120 mV, at 20-mV steps. The dashed line shows zero-current level. (*C*) Current amplitude (pA/pF) measured at the beginning [▲, △] and end [▼, ▽] of the voltage pulse and plotted *vs.* voltage in two groups of cells as *A* and *B*. Mean values ± SEM for 10 control [△, ▽] and cyclic AMP-stimulated [▼, ▲] cells.

a holding potential of −40 mV, a value which is close to the resting membrane potential of unstimulated Leydig cells (Duchatelle & Joffre, 1990) (Fig. 1*A*). An inward current (holding current) averaging −113.1 ± 26.7 pA (n = 10) was continuously recorded at the holding potential. Hyperpolarizing or depolarizing voltage pulses (375 msec) elicited time-independent currents. No tail current was measured on clamping back to −40 mV. Mean current-voltage curves of the instantaneous current and of the current at the end of pulses, drawn from 10 cells, were quite linear. They only showed a slight inward rectification for potentials more negative than −60 mV (Fig. 1*C*). This current reversed at 0 mV.

Current traces were then recorded in cells dialyzed with 0.1 mM cyclic AMP-Na salt, added to the ATP-Mg-enriched solution. Within 5 sec of achieving the whole-cell recording configuration, the magnitude of both inward and outward currents increased progressively. A plateau response was always recorded within 1–5 min following the exposure to cyclic AMP, so that the inward holding current averaged −351.4 ± 46.6 pA (n = 10; $P < 0.01$). Long (375 msec)-hyperpolarizing or depolarizing voltage steps from −40 mV to voltages ranging from −120 to +40 mV only elicited time-independent currents. For potentials over +60 mV, however, the currents peaked instantaneously after applying the voltage steps and then decayed with time (Fig. 1*B*). Tail currents were measured upon repolarization to −40 mV. In any given cells, the tail currents were increased and the rate of decay was always faster at +120 than at +60 mV. The mean current-voltage relationship averaged from 10 cells is illustrated in Fig. 1*C*. Instantaneous current was quite linear from −120 to −40 mV, then showed a strong outward rectification for potentials over −40 mV. The reversal potential of this cyclic AMP-activated current is close to 0 mV.

In order to investigate whether the currents elicited in unstimulated cells might directly contribute to the effects of cyclic AMP, 500 μM (8-[4-chlorophenylthio]cyclic AMP, PSCl-cyclic AMP), a cyclic AMP analogue which diffuses through the membranes of intact cells, was added to the external medium perifused on the test cell. Figure 2 illustrates one of these experiments (n = 4). Depolarizing voltage steps to +80 mV were applied, every 10 sec, from a holding potential of −40 mV, to cells which were initially perifused with the control medium. Within 4 min of achieving the whole-cell recording configuration, the holding and the instantaneous outward currents swiftly increased and then slightly decreased to reach a steady-state level. Both currents remained constant more than 30 min, indicating that the pipette solution had equilibrated with the cell's cytoplasm. This run-up/run-down phenomenon was a systematic finding in control cells, independently of the presence of internal ATP, but did not appear in cells dialyzed with ATP and cAMP (Duchatelle & Noulin, *unpublished data*). Within 2 min following the exposure to PSCl-cyclic AMP, the outward and the holding currents increased simultaneously. Concomitantly, the current traces at +80 mV progressively decayed with time (Fig. 2*B*). This long-lasting response appeared slowly reversed upon withdrawal of PSCl-cyclic AMP.

In the presence of cyclic AMP, the current traces decayed with time, at potentials over +60 mV, and were always followed by tail currents on clamping back to the holding potential (Fig. 1*B*). We investigated the effects of the duration of depolarizing pulses on this tail current. Figure 3*A* illustrates the effects of different pulse durations when

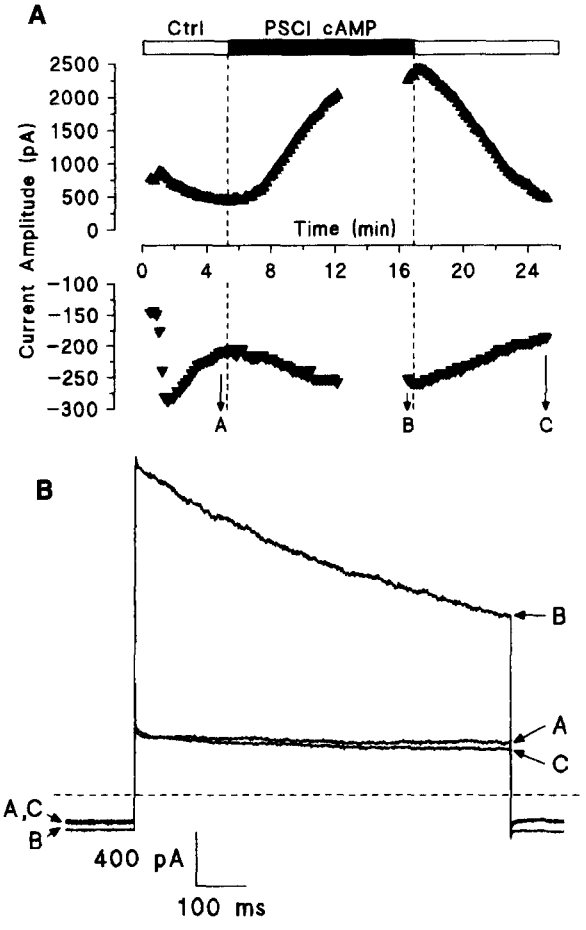

Fig. 2. Effect of 500 μM 8-[4-Chlorophenylthio]cyclic AMP, PSCl-cyclic AMP) perifusion on whole-cell currents from a cell under control conditions. (*A*) Current traces at −40 mV (holding potential) [▼] and +80 mV [▲], in response to 375-msec pulses, applied every 10 sec. (*B*) current traces recorded before (*A*), during (*B*) and after (*C*) the perifusion with PSCl-cyclic AMP. The dashed line shows zero-current level.

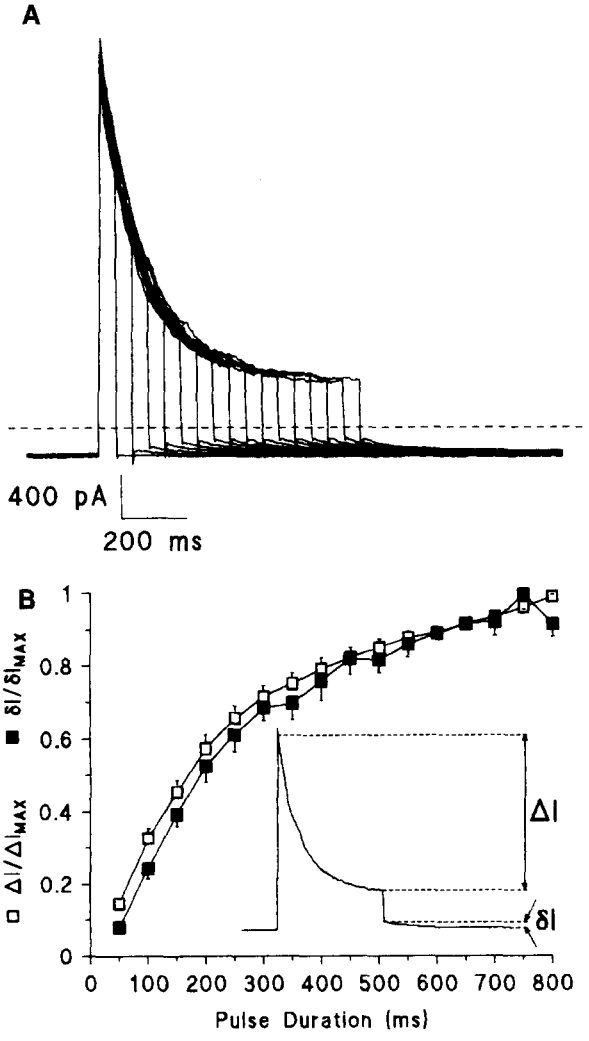

Fig. 3. Effect of pulse duration on whole-cell currents from a cell in the presence of cyclic AMP. (*A*) Pulses were applied every 10 sec from −40 mV (holding potential) to +120 mV by increments of 50 msec. The dashed line shows zero-current level. (*B*) Normalized amplitudes (*see* inset) of outward [□] and inward [■] currents *vs.* pulse duration. Mean values ± SEM for 16 cells.

stepping from a holding potential of −40 to +120 mV, on the subsequent tail currents at −40 mV. The magnitude of the outward currents measured at the end of the pulses decreased, and that of the inward tail currents increased, as the duration of the +120-mV test pulses was longer. The data shown in Fig. 3*B* quantify these observations for 16 cells. The increase in the tail current amplitudes at −40 mV paralleled the decrease of outward current at +120 mV when the +120-mV test pulses were increased in duration.

Voltage-Clamp Experiments at a Positive Holding Potential

The results in Fig. 3 strongly suggest that the tail currents were related to an inward current activated by hyperpolarization, and deactivated by clamping to positive potentials over +60 mV. Evidence for this was obtained from experiments illustrated in Fig. 4, where the holding potential was held at +60 mV and voltage steps to −60 mV were applied for various durations. On clamping to +120 mV, outward tail currents were recorded. The time courses of current activation and of the envelopment of instantaneous outward tail currents were compared (Fig. 4*C* and *D*). It can be seen that the envelopment of tail currents matches closely the time course of the onset of inward current. The time constants of activation and of the envelopment of deactivation were fitted by a double exponential. The time constants of activation, at +60 mV, were 330 and 3,422

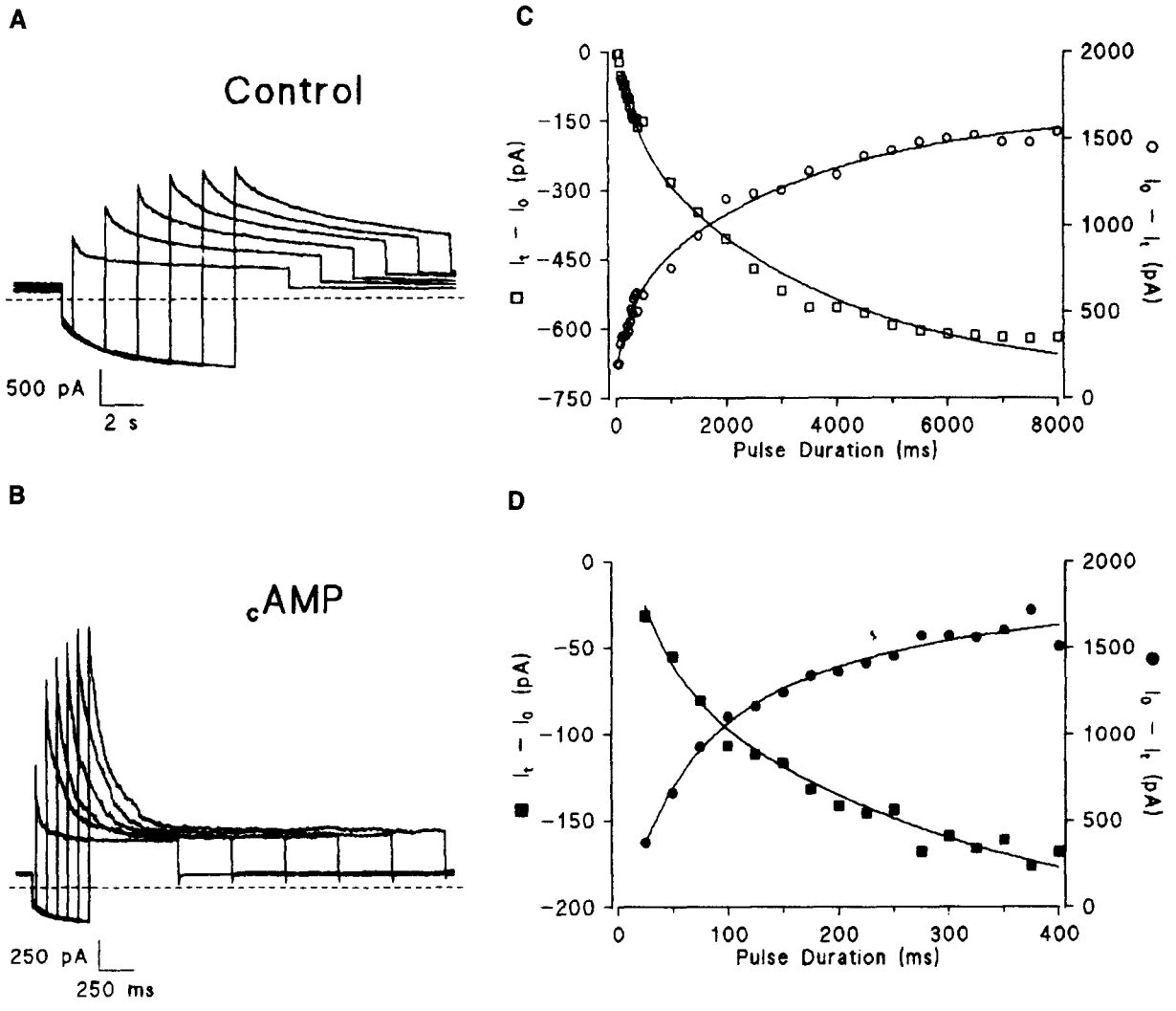

Fig. 4. Effect of cyclic AMP on kinetic properties of hyperpolarization-activated inward currents. (*A* and *C*) control cell; (*B* and *D*) cyclic AMP-stimulated cell. (*A* and *B*) six different current traces recorded at various intervals. Current was activated by hyperpolarization from a holding potential of +60 to −60 mV and was deactivated at the potential of +120 mV. The dashed line shows zero-current level. (*C* and *D*) Time courses of current activation [□, ■] and of the envelope of deactivation [○, ●]. Both curves are well fitted by a double exponential (*see text*).

msec while the time constants of the deactivation, envelopment at +120 mV, were 331 and 3,397 msec in control cells. They were greatly decreased in the presence of internal cyclic AMP (33 and 287 msec; 51 and 250 msec, respectively).

Voltage- and Cyclic AMP-Dependence of the Inward Current

Steady-State Parameters of Current Activation

In these experiments, the holding potential was held at +60 mV and the whole-cell currents were analyzed during hyperpolarizations applied from +60 mV. Figure 5*A* shows superimposed current traces elicited by hyperpolarizing or depolarizing voltage pulses. An outward holding current, averaging 53 ± 10 pA (n = 13), was recorded. Depolarizations beyond +60 mV induced time-independent outward currents. In contrast, hyperpolarizations lasting for 7 sec beyond 0 mV activated an inward current, which increased with time to reach a steady-state level. Increasing the hyperpolarization to −120 mV speeded up the time course of currents and enhanced their amplitude. Mean steady-state currents averaged from different cells are plotted against voltages in Fig. 6*A*. The steady-state current reversed near

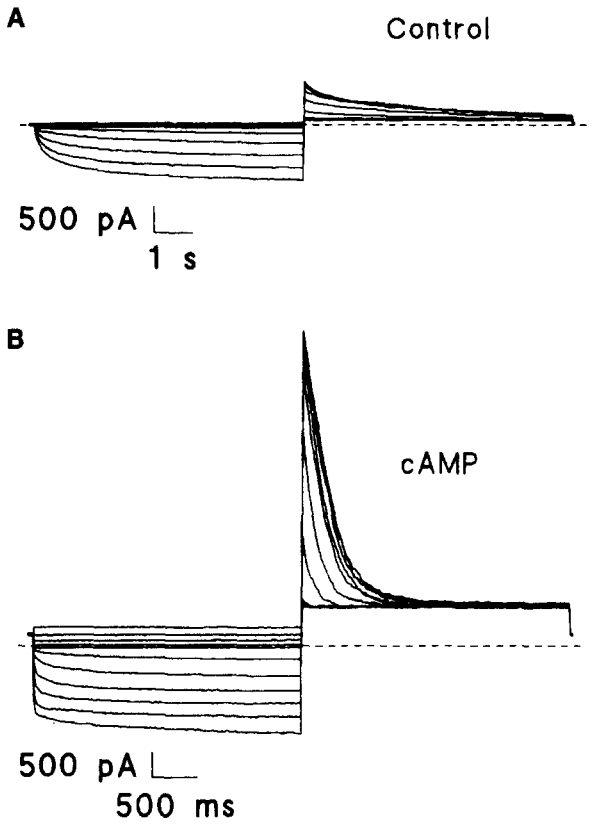

Fig. 5. Whole-cell currents from cells under control conditions (*A*) and in the presence of cyclic AMP (*B*). Superimposed current traces recorded with depolarizing and hyperpolarizing pulses between +80 and −120 mV from a holding potential of +60 mV, at +20-mV increments. Step durations were held for 7 sec (*A*) and 3 sec (*B*). They were enough to reach steady-state levels of current. Membrane was then clamped back to +120 mV for 7 sec (*A*) and 3 sec (*B*). The dashed line shows zero-current level. Recordings are representative of six (*A*) and eight (*B*) cells. Stimulation frequency: 0.1 Hz (*A*) and 0.03 Hz (*B*).

0 mV, showing a strong inward rectification for potentials below 0 mV. In these experiments, the current activation was always followed by a depolarization to +120 mV, which led to an instantaneous rapidly deactivating outward current. The amplitude of the tail currents was normalized and plotted against the prepulse potential (Fig. 6*B*). The activation curve extended from +60 mV [0] to −120 mV [1]. It was fitted according to the following equation:

$$A = 1/[1 + \exp\{(V\text{-}V_{0.5}/S\}],$$

where A is the activation parameter, V is the membrane potential, $V_{0.5}$ is the potential of the half-maximum activation and S is the slope factor of the curve. In control conditions, S averaged 20 mV and $V_{0.5}$ was close to −40 mV.

Effects of Cyclic AMP

The sensitivity of the hyperpolarization-activated currents to this nucleotide was first studied by dialyzing the cells with 100 μM cyclic AMP (Fig. 5*B*). In this case, the holding current at +60 mV was enhanced (169 ± 18 pA; $n = 15$; $P < 0.01$). Positive voltage pulses still induced time-independent outward currents, which showed an increased amplitude. Inward currents were also recorded in response to hyperpolarizing pulses. In a first approximation, their steady-state amplitude was quite similar to that of the control values, while the kinetics of their activation appeared to be accelerated at all negative voltage pulses. Increasing the hyperpolarization to −120 mV speeded up the time course of the currents.

Cyclic AMP flattened the *I-V* curve (Fig. 6*A*). The mean amplitude of the outward current ($n = 6$) was increased between 0 and +80 mV. The inward current was unchanged below −60 mV, but was enhanced between 0 and −60 mV. The reversal potential was maintained at 0 mV. Cyclic AMP did not alter the threshold potential of activation (Fig. 6*B*). It shifted the mid-activation curve ($V_{0.5}$) by about 24 mV, and induced an increase of its steepness (S near 16 mV).

These cyclic AMP-induced changes could be mimicked, although to a lesser extent, by applying 500 μM PSCl-cyclic AMP to the external medium (Fig. 7).

Steady-State Parameters of Current Deactivation

Figure 5 suggests a steady-state conductance increase during current activation by the membrane potential. This is illustrated in Fig. 8*A*, where the steady-state conductance is plotted against membrane potential. In control cells, this conductance was progressively enhanced by hyperpolarizations from +60 to −120 mV. This effect was further increased by 0.1 mM cyclic AMP, in the range of +20 to −40 mV. The maximal steady-state conductance appeared to be similar in unstimulated and cyclic AMP-stimulated cells.

Figure 8*B* illustrates the relationships between the instantaneous (outward) conductance at +120 mV and the prepulse potential value. This shows the progressive increase in this conductance in control cells and demonstrates its substantial increase in cyclic AMP-stimulated cells. Despite similar steady-state (inward) conductances recorded in both cells below −80 mV, the instantaneous (outward) conductance of stimulated cells was 3.5 times higher than that of control cells.

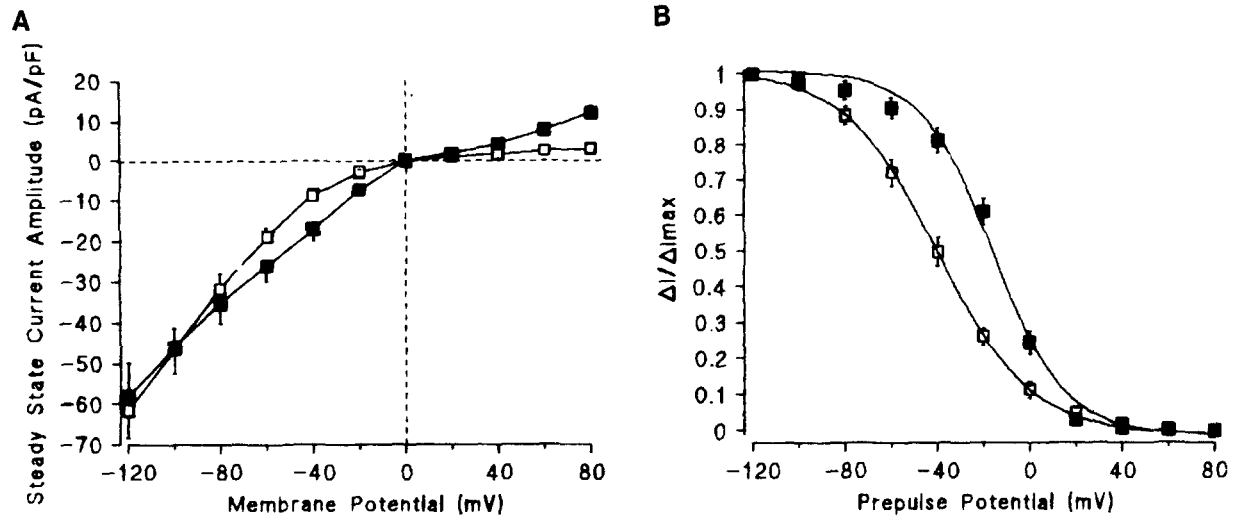

Fig. 6. Effect of cyclic AMP on the amplitude and the steady-state activation of whole-cell current from cells under control conditions (□) and in the presence of cyclic AMP (■). (*A*) Current amplitudes (pA/pF) measured at the end of the voltage pulse are plotted *vs.* potential in two groups of cells. (*B*) Activation curve of hyperpolarization-activated inward current. The normalized amplitudes of the tail current are plotted *vs.* membrane potential (prepulse potential). (*A* and *B*) Mean values ± SEM for six control [□] and eight cyclic AMP-stimulated [■] cells.

Figure 9 confirms these findings. Inward current, which was previously activated by hyperpolarizations to −120 mV, was then deactivated by clamping back to different potentials beyond 0 mV. The characteristics of the corresponding current-voltage curves were similar to those of experiments in which depolarizations were applied from a holding potential of −40 mV (Fig. 1).

Kinetics of Current Activation and Deactivation

The activation curve was steepened by dialysis with cyclic AMP (Fig. 6*B*). These results suggest that the kinetics of activation is different between the two groups of cells. To test this hypothesis, the time constants for current activation were calculated from current traces shown in Fig. 5*A* and *B*. Current traces could be well fitted by a double exponential. Both the fast and slow components were weakly voltage dependent in control cells (Table and Fig. 10). They were greatly decreased, and the slope of the voltage dependence increased, in the presence of cyclic AMP ($P < 0.01$).

The kinetics of current deactivation was estimated from current traces such as those displayed in Fig. 9*A* and *B*. The current deactivation was well fitted by a single exponential function. The rate constant had a high value and was voltage independent in control cells, but was much lower and strongly voltage dependent in stimulated cells ($P < 0.01$) (Table and Fig. 10).

Ionic Selectivity and Pharmacology

Reversal Potential

The hyperpolarization-induced inward current slowly deactivated below +60 mV, making it difficult to measure the reversal potential by the standard tail current procedure. Since the inward current did not inactivate, we have applied a voltage ramp (dV/dt = 1.6 V/sec) in which the hyperpolarization-induced current was first activated by a long square pulse to −100 mV. Examples of these *I-V* curves are shown in Fig. 11. To demonstrate the ionic nature of the current flowing through membrane channels, we replaced either cesium or chloride ions. In the latter case, the liquid junction potential induced by substituting glutamate for chloride ions was measured (+6.5 mV) and canceled. Cells were first bathed in control medium, then perifused with test solutions. The *I-V* relationships for the inward current were essentially similar to those obtained by the square pulse stimulus, with a more pronounced outward rectification recorded at positive potentials in some cyclic AMP-stimulated cells (Fig. 11*D*). The reversal potential (E_{rev}) obtained from cyclic AMP-stimulated cells bathed in control medium was:

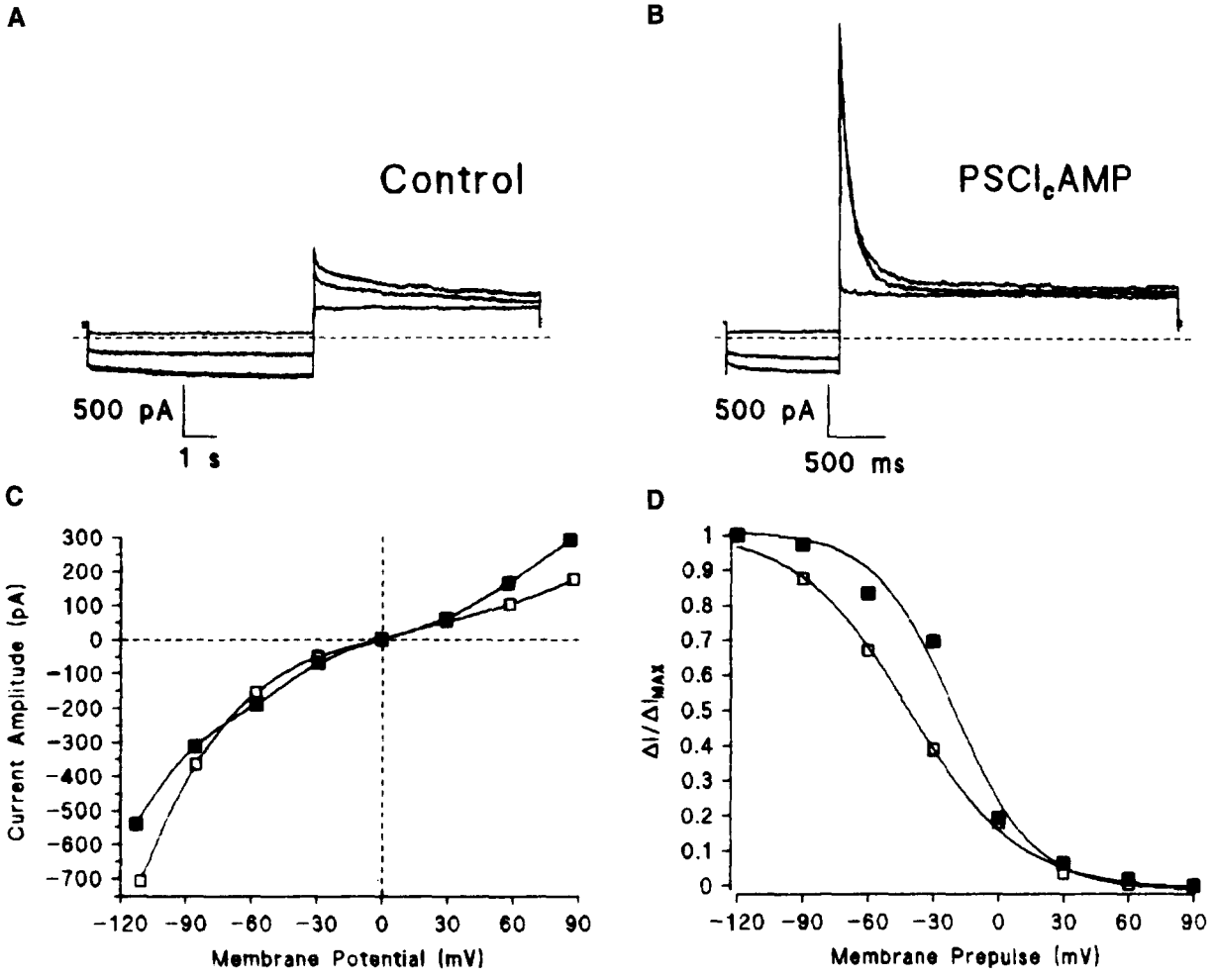

Fig. 7. Effects of 500 μM 8-(4-Chlorophenylthio)cyclic AMP on the amplitude (*C*) and the steady-state activation (*D*) of whole-cell currents. Whole-cell currents under control conditions (*A*) and at the plateau response to cyclic AMP (*B*). Superimposed current traces recorded at +30, −60 and −90 mV, as in Fig. 5. (*C*) Current amplitudes measured at the end of the voltage pulse are plotted *vs.* potential. (*D*) Activation curve of the hyperpolarization-activated inward current. The normalized amplitudes of the tail current are plotted *vs.* membrane potential (prepulse potential). (*C* and *D*) control [□] and cyclic AMP-stimulated [■] cell.

−1.9 ± 1.0 mV (n = 4). Neither E_{rev} (−1.5 ± 1.1 mV; n = 4), nor the slope conductance were affected by the complete replacement of cesium chloride with equimolar TEA-chloride salt (Fig. 11*C*). By contrast, the cesium chloride substitution by cesium glutamate, which induced an increase in E_{Cl} from 0 to +50.9 mV, shifted E_{rev} (+28.5 ± 4.1 mV; n = 5; $P < 0.01$) and decreased the slope conductance (Fig. 11*D*).

Similar results were obtained in control cells (Fig. 11*A* and *B*). E_{rev} was −5.4 ± 1.3 mV (n = 10) in control medium. Neither E_{rev} (−5.7 ± 1.5 mV; n = 10), nor the slope conductance were affected by the complete replacement of cesium ions with equimolar TEA-chloride salt (Fig. 11*A*). By contrast, E_{rev} was shifted (+25.5 ± 3.1 mV; n = 6; $P <$ 0.01) by the cesium chloride substitution by cesium glutamate (Fig. 11*B*).

Sensitivity to Chloride Channel Blockers

Specific channel blockers are extensively used to identify a membrane current. Since the responses to TEA and glutamate did not differ between control and cyclic AMP-stimulated cells, we decided to examine the effects of a disulfonic-stilbene acid derivative (DIDS [4,4′-diisothiocyanatostilbene-2,2′-disulfonic acid]) and of two carboxylic acid analogues (9-AC [anthracene-9-carboxylic acid] and DPC

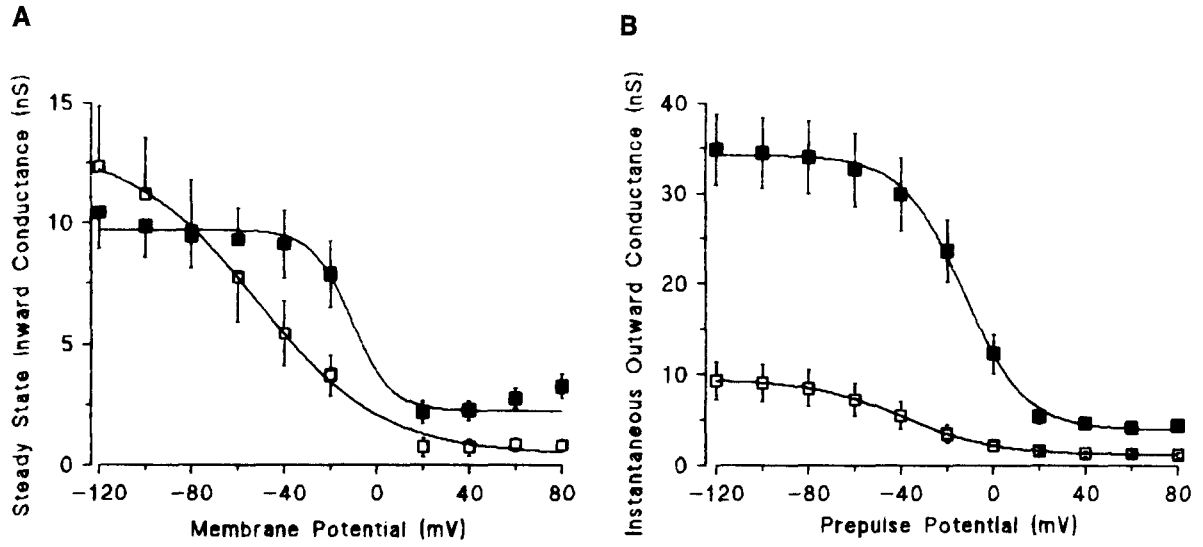

Fig. 8. Effects of cyclic AMP on steady-state (*A*) and instantaneous (*B*) conductances from cells under control conditions [□] and in the presence of cyclic AMP [■]. Data were obtained from Fig. 5. The steady-state conductance, calculated from $G_x = I_x/(V_x - E_{eq})$, and the instantaneous conductance, calculated from $G_{120} = I_{120}/(V_{120} - E_{eq})$, are plotted *vs.* membrane potential (prepulse potential). They are expressed as mean values ± SEM for six control [□] and eight cyclic AMP-stimulated [■] cells.

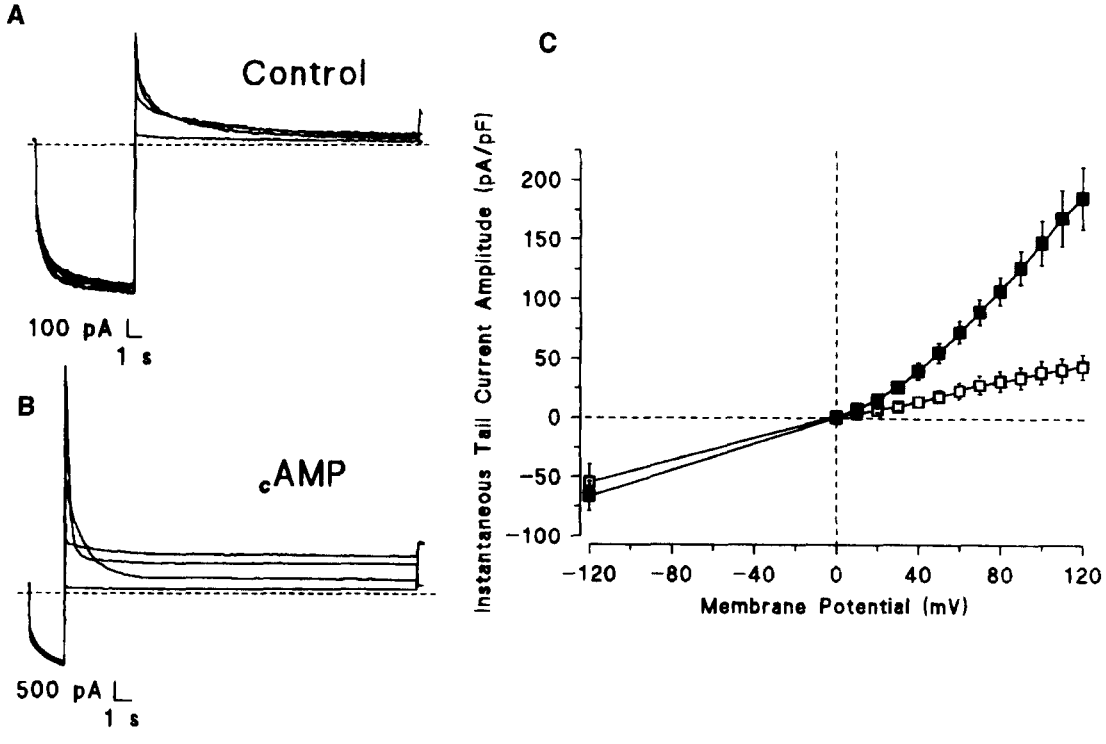

Fig. 9. Effect of cyclic AMP on instantaneous outward currents from cells bathed in symmetrical cesium chloride and dialyzed with 3 mM ATP [□] and 0.1 mM cyclic AMP [■]. (*A–B*) Current traces recorded in a control cell [upper panel] and in the presence of 0.1 mM cyclic AMP [lower panel]. Four superimposed current traces recorded with hyperpolarizations from +60 to −120 mV. Membrane was then clamped back to +10, +50, +80 and +120 mV. The dashed line shows zero-current level. Recordings are representative of six (*A*) and five (*B*) cells. (*C*) Instantaneous current amplitudes (pA/pF) are plotted *vs.* membrane potential in two groups of cells. Data are expressed as mean ± SEM for six control [□] and five cyclic AMP-stimulated [■] cells.

Table. Effect of cyclic AMP on time constants of activation and deactivation

	Time constant of activation (msec)				Time constant of deactivation (msec)	
	−40 mV		−100 mV		+60 mV	+100 mV
	τ fast	τ slow	τ fast	τ slow	τ	
0 cAMP	491 ± 113 (5)	4,103 ± 714 (6)	383 ± 45 (11)	2,791 ± 264 (11)	2,316 ± 293 (6)	2,399 ± 668 (6)
+ cAMP	38 ± 7 (14)	364 ± 44 (14)	8 ± 1 (16)	180 ± 43 (16)	1,863 ± 172 (5)	423 ± 77 (5)

Hyperpolarization-activated inward currents were obtained from cells bathed in symmetrical cesium chloride and dialyzed with 3 mM ATP alone [0 cAMP] and 0.1 mM cyclic AMP [+ cAMP]. The time constants of activation and deactivation are obtained from exponential fits of recordings as in Figs. 5, 9. They are expressed as mean values ± SEM for (n) values.

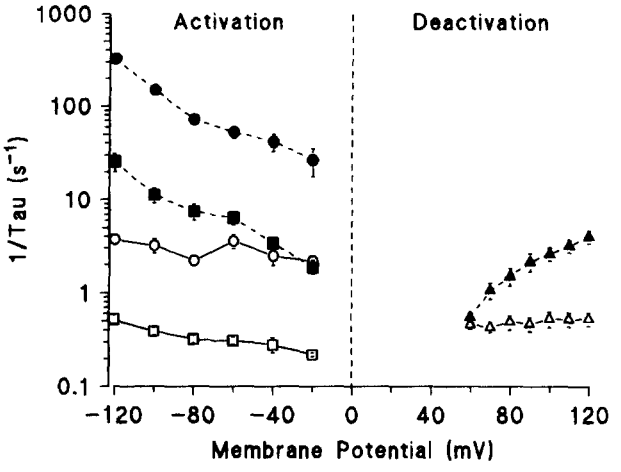

Fig. 10. Effects of cyclic AMP on kinetic properties of hyperpolarization-activated inward current. Cells were under control conditions [open symbols] and in the presence of cyclic AMP [filled symbols]. The rate constants of activation and deactivation are plotted *vs.* membrane potential in two groups of cells on a semilogarithmic graph. Data are obtained from exponential fits of recordings. They are expressed as mean ± SEM for n cells given in the Table. Activation rate constants were calculated from current traces illustrated in Fig. 5; deactivation rate constants from current traces in Fig. 9.

[diphenylamine-2-carboxylic acid]) on currents induced by hyperpolarization in cyclic AMP-dialyzed cells. Figure 12 shows representative *I-V* curves obtained in the presence of these three channel blockers. They demonstrate that an external perifusion with 1 mM DIDS (n = 3), dissolved in the control medium, or with 1 mM 9-AC (n = 3), or with 1 mM DPC (n = 3), dissolved in DMSO then in the control medium (2% DMSO), inhibited the currents. The inhibition was fast with DIDS and was delayed (from 1 to 2 min) with the carboxylic acid derivatives. The steady-state inward currents were largely decreased in the presence of DIDS and DPC (Fig. 12*A* and *C*). They were little affected by 9-AC (Fig. 12*B*). Despite this difference, all drugs substantially decreased the instantaneous outward currents recorded on clamping back to +120 mV. Consequently, the corresponding *I-V* curves were differently affected.

Discussion

Identification of a Hyperpolarization-Activated Chloride Conductance in Leydig Cells

A cyclic AMP-dependent chloride conductance is involved in the response of rat Leydig cells to luteinizing hormone (LH). (Duchatelle & Joffre, 1990). Recently, the currents induced by depolarizations and their sensitivity to chloride channel blockers have been compared in cells dialyzed either with cyclic AMP or with calcium (Noulin & Joffre, 1992*a*). In cells dialyzed with cyclic AMP, depolarizations from a holding potential of −40 mV, the value of the resting membrane potential of Leydig cells, induced outward currents peaking instantaneously and decaying with time at voltages above +60 mV. This current displayed a strong outward rectification for potentials beyond 0 mV. Similar results have now been obtained in cells dialyzed with cyclic AMP, and bathed in a cesium chloride solution identical to the pipette solution (Fig. 1*B* and *C*).

Since this current reversed near E_{Cl} and was inhibited by DIDS and SITS, we concluded (Duchatelle & Joffre, 1990; Noulin & Joffre, 1992*a*) that a

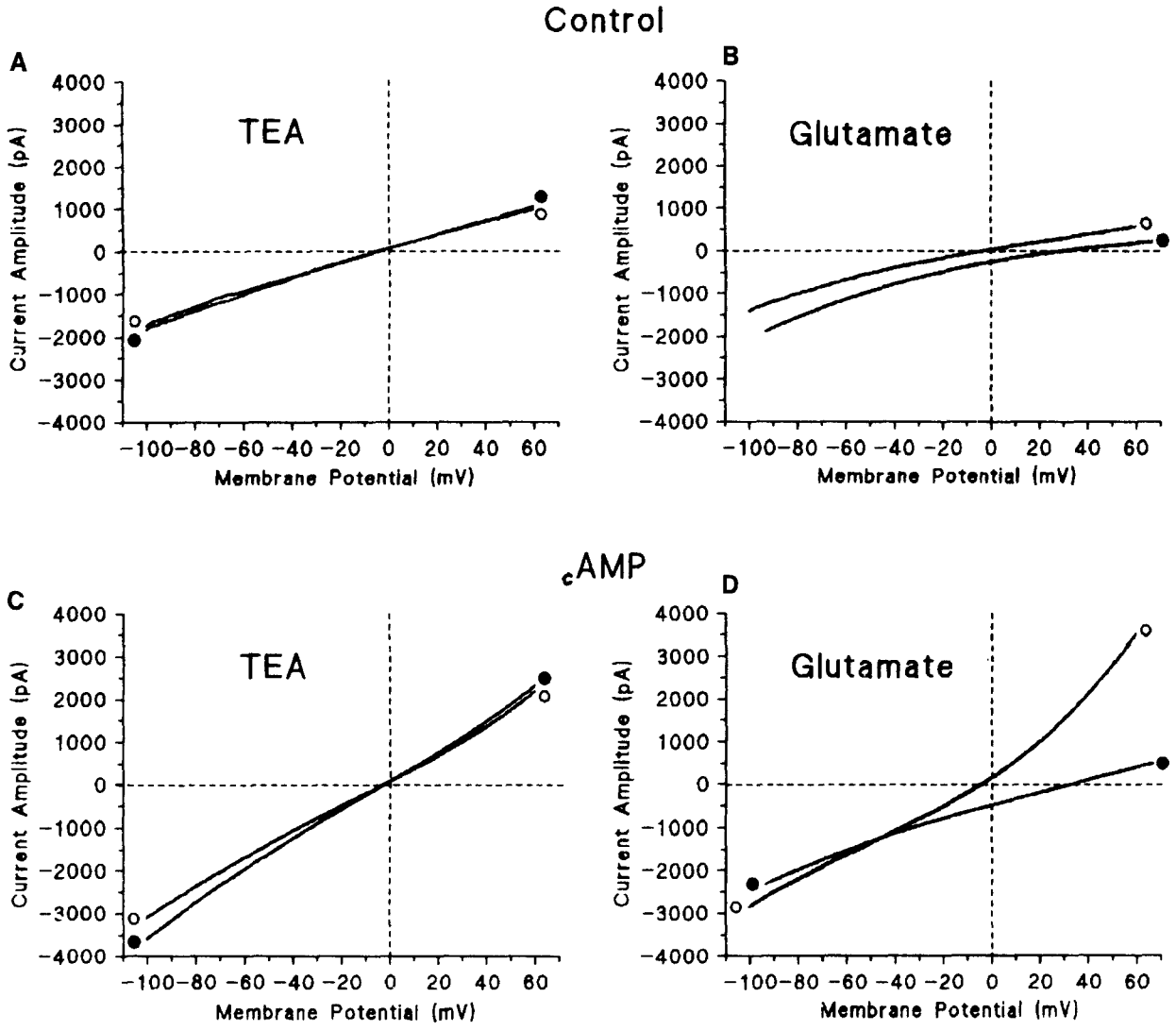

Fig. 11. Effects of external TEA (*A* and *C*) and glutamate (*B* and *D*) on the current-voltage relationships measured by ramp voltage pulses in cells under control conditions (*A* and *B*) and in the presence of cyclic AMP (*C* and *D*). Holding potential was set at +60 mV. Inward current was first activated by a 3-sec long square pulse to −120 mV and a ramp pulse (dV/dt = 1.6 V/sec) was then applied. (*A* and *C*) *I-V* relationships in the control medium [○] and in the presence of 150 mM external TEA-Cl [●]. (*B* and *D*) *I-V* relationships in the control medium [○] and in the presence of 130 mM external Cs-glutamate [●] corrected for the liquid junction potential (*see text*). These curves are representative of four different experiments.

cyclic AMP-activated chloride conductance is present in the membrane of Leydig cells, as described in many epithelial and nonepithelial cells (Matthews, Neher & Penner, 1989; Mc Cann, Li & Welsh, 1989, Solc & Wine, 1991; Wine et al., 1991). We initially considered that this conductance is first activated by depolarization, and that voltage jumps to +60 mV or more subsequently inactivated the channels. However, the observation of a sustained holding current (Fig. 1) now leads us to consider instead a conductance which is activated at the negative potential, and subsequently deactivated on clamping to positive potentials. Two groups of data support this proposal. First, when stepping the voltage to +120 mV for different durations, the longer the voltage is maintained at +120 mV, the greater the current decays and the values of the tail current observed upon returning to −40 mV increases (Fig. 3). Second, the time course of current activation upon stepping to −60 mV matches closely that at the onset of instantaneous outward tail currents (Fig. 4). Thus, we conclude by confirming that a cyclic AMP-dependent and hyperpolarization-activated chloride conductance is present in the membrane of Leydig cells, as it is in the epithelial cells from the human airways (Mc Cann et al., 1989).

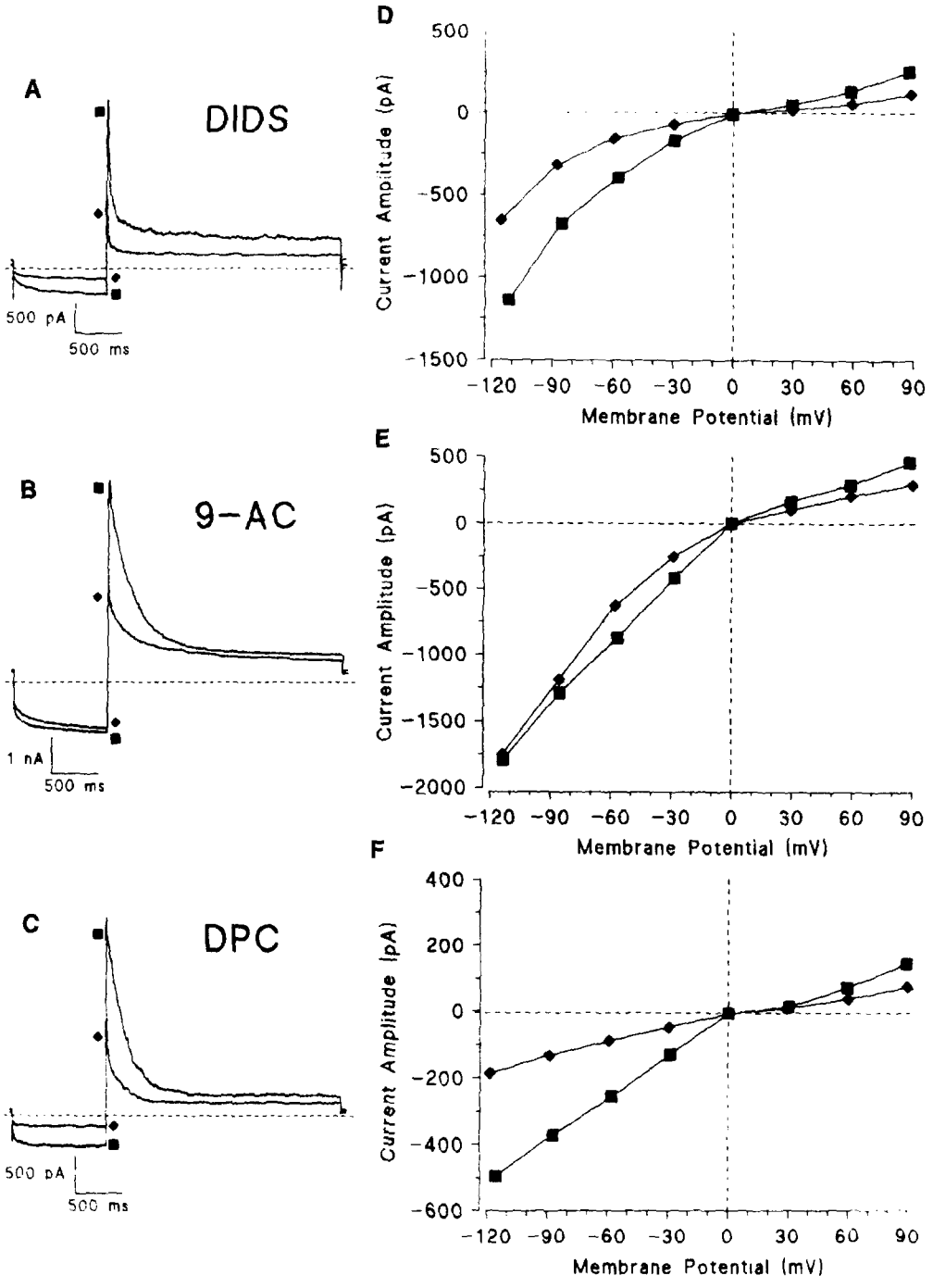

Fig. 12. Effect of three chloride channel blockers on hyperpolarizarion-activated inward current in cells bathed in the presence of cyclic AMP. (*A–C*) Current traces recorded in the control medium [■] and in the presence of 1 mM external blocker [◆] with hyperpolarizing pulses at −90 mV for 1 sec from a holding potential of +60 mV and clampled back to +120 mV for 2.5 sec. The dashed line shows zero-current level. (*D–F*) Fully activated current *vs.* membrane potential drawn for left panel. These curves are representative of three different experiments. (*A* and *D*) DIDS; (*B* and *E*) 9-AC; (*C* and *F*) DPC.

To study this conductance, the holding potential was held at +60 mV, the value at which the time-dependent decay of outward current was recorded, and the pulse duration was increased from 375 msec to 3 or 7 sec. Current relaxations were then revealed (which are not apparent in most traces of Fig. 1; *see* Fig. 5). Hyperpolarizations below 0 mV induced the activation of time-dependent inward currents, which increased in amplitude as a function of time to reach a steady-state level (Fig. 5). Large hyperpolariza-

tions speeded up the time course of this time-dependent component and increased the steady-state amplitude. Consequently, the *I-V* curves showed inward rectification properties (Fig. 6*A*). Moreover, clamping to +120 mV was always followed by outward tail currents, which peaked instantaneously and then decayed with time. These currents resembled the outward currents recorded in the first part of this study, when cells were depolarized from a holding potential of −40 mV (Fig. 1).

The time course, the voltage dependence and the inward rectification properties of this current resemble qualitatively those of the well-known pacemaker current (I_f or I_h) of sino-atrial or Purkinje cells from mammalian heart and of frog sinus venosus cells (Callawaert, Carmeliet & Vereecke, 1984; DiFrancesco et al., 1986; Hagiwara & Irisawa, 1989; Bois & Lenfant, 1990; Van Ginneken & Giles, 1991). Both exhibited a time- and voltage-dependent activation and showed large outward tail currents upon returning to a depolarized level. But these two currents are distinct in many respects. In this study, the currents were recorded in a solution of cesium chloride which strongly blocks I_f, and without potassium and sodium ions, known to be involved in the pacemaker current (*see review*, DiFrancesco, 1985). They were insensitive to cesium substitution for TEA (Fig. 11*A* and *C*). Their reversal potentials were quite near E_{Cl} and were shifted with the chloride concentration gradient, providing strong evidence for currents which were mainly carried by chloride ions (Fig. 11*B* and *D*). These currents were also inhibited by nonspecific and specific chloride channel blockers (Fig. 12) (Gögelein, 1988). Further differences were also apparent from kinetics of activation and deactivation. Although the Leydig cell conductance and I_f were fully activated near −120 mV, their thresholds of activation were near +60 and −70 mV, respectively. The activation and deactivation of I_f follow a single exponential (DiFrancesco, 1984). In contrast, the deactivation of the conductance in Leydig cells varied as a single exponential, whereas the activation curve was well fitted with a double exponential. Consequently, all these findings agree with the presence of a hyperpolarization-activated chloride conductance different from I_f in the membrane of mature rat Leydig cells.

Voltage-clamp experiments carried out on whole cells have previously shown hyperpolarization-activated inward chloride currents in *Aplysia* neurons (Chesnoy-Marchais, 1982, 1983; Lotshaw & Levitan, 1987), *Xenopus* oocytes (Parker & Miledi, 1988), a human colonic cell line (T84) (Worrel et al., 1989) and hippocampal neurons (Madison, Malenska & Nicoll, 1986; Mager, Ferroni & Schubert, 1990). Moreover, instantaneous outwardly rectifying currents resembling the present outward currents have been recorded in cells of the human airway epithelium, in T84 cells and in human sweat glands and trachea (Mc Cann et al., 1989; Worrel et al., 1989; Solc & Wine, 1991; Valverde, Mintenig & Sepúlveda, 1991). These currents show several properties in common with the chloride current in Leydig cells. They are activated by cyclic AMP and blocked by disulfonic stilbene and carboxylic acids. Furthermore, they demonstrate outward rectification properties and an important decay with time for positive potentials. In these latter cells, the currents are related to an outward rectifying, depolarization-induced chloride channel (ORDIC) (Mc Cann et al., 1989; Solc & Wine, 1991). All these considerations might argue for an "ORDIC channel" type in the membrane of Leydig cells, a channel which is activated by hyperpolarization and deactivated by strong depolarization.

Low outward and holding currents were measured in response to depolarizations, applied to control Leydig cells from −40 mV (Fig. 1*A*). In these cells, applying hyperpolarizations from +60 mV beyond 0 mV, induced inward currents, and clamping back to +120 mV was followed by outward tail currents which peaked instantaneously, then decayed with time. This current resembled qualitatively those recorded in the presence of cyclic AMP and was insensitive, too, to cesium replacement by TEA (Fig. 11*A*). Its reversal potential was near E_{Cl} and shifted with the chloride concentration gradient (Fig. 11*B*). That is in agreement with the view that cyclic AMP did not activate a new chloride conductance, but rather modulated a background chloride conductance. This proposal was confirmed by the progressive increase in the outward and inward currents observed when cells were perifused with (8-[4-Chlorophenylthio]cyclic AMP, PSCl-cyclic AMP) (Figs. 2 and 7).

Modulation of the Background Chloride Conductance by Cyclic AMP

Our conclusion of similarities between this current and I_f was strengthened by the fact that both are sensitive to cyclic AMP. The effects of this nucleotide on I_f have been extensively analyzed in cardiac cells (Tsien, 1974; Callawaert et al., 1984; DiFrancesco et al., 1986; Hagiwara & Irisawa, 1989; DiFrancesco & Tortora, 1991). In Leydig cells, as in cardiac cells, cyclic AMP shifts the steady-state activation curve to a more positive potential and increases the steepness of the activation curve without modifying the threshold of activation.

Cyclic AMP strengthened the steady-state current-voltage relationship. With maximal responses, the *I-V* curves were more frequently linear in the range of 0 to −120 mV. This response varied from cell to cell and was probably dose dependent. Although no dose-dependent effect has yet been investigated, curvilinear *I-V* curves were nevertheless observed in the presence of 500 μM PSCl-cyclic AMP.

On Leydig cells, cyclic AMP increased the inward current activation by acting on the current kinetics rather than on its amplitude (Fig. 6). This nucleotide increased the current toward the half-activation range and accelerated the rate of current activation on pulsing to more negative levels. Both activation constants were increased and became highly voltage dependent as the membrane potential was changed toward more negative values. These results largely agree with a control of the chloride conductance in Leydig cells quite similar to I_f in cardiac cells. Cyclic AMP might increase the inward chloride current by increasing either the number of active channels or their mean open time.

The rate constants of deactivation were largely increased and became voltage dependent in the presence of cyclic AMP. Surprisingly, despite quite similar "inward" conductances in control and in cyclic AMP-dialyzed cells, the instantaneous outward currents and the related "outward" conductance were much higher in the presence of cyclic AMP. (Figs. 8*B* and 9). Two hypotheses can be put forward to explain these results. Depolarizations might induce either an activation of a new outward chloride current, or an increase in the outward rectification. The first proposal implies that this new current is activated instantaneously, and subsequently inactivated. As a consequence, such a hypothesis leads us to consider the decrease of current that follows the activation from −40 to +120 mV, as the sum of two currents corresponding to the deactivation of the hyperpolarization-activated current and the inactivation of a depolarization-induced current. However, that is not the case since the current deactivation is well fitted by a single exponential and since the time course of the envelopment of the instantaneous outward tail current and that of the onset of current activation are the same (Fig. 4). Moreover, when stepping the voltage to +120 mV for different durations, the longer the voltage was maintained at +120 mV, the more the current decayed and the values of the tail current increased upon returning to −40 mV (Fig. 3). Moreover, the activation curve reflects the *I-V* curve of the hyperpolarization-activated current exactly (Fig. 6), a fact which is in agreement with the view (second proposal) that cyclic AMP increases the depolarization-induced outward rectification subsequently to an increase in the "outward" unitary conductance of channels.

Physiological Role of the Hyperpolarization-Activated Chloride Conductance

This conductance is involved in the responses to LH, to hCG and GTP stimulation (Duchatelle & Joffre, 1990). A membrane depolarization was measured when Leydig cells were exposed to hCG or dibutyryl cyclic AMP (Joffre et al., 1984), a result which may now be explained by an increase in the chloride conductance allowing chloride ions to exit the cell. Recently, Choi and Cooke (1990), on the basis of our preliminary data (Duchatelle & Joffre, 1987), have demonstrated an active chloride pathway in the membrane of Leydig cells that is involved in low LH-stimulated testosterone secretion. But, if these results agree with a role of chloride ions in the physiology of LH-stimulated Leydig cells, the coupling between this conductance and steroidogenesis remains to be specified. Additional experiments are now required to investigate the role of this chloride conductance in stimulus-response coupling.

The authors thank Pierrette Régondaud, Jean-Pierre Poindessault and Jacques Alix for technical assistance. They are indebted to J. Délèze, J. Lenfant and A. Marty for helpful comments on the manuscript. This work was supported by grants from the CNRS and the DRED du Ministère de l'Education Nationale.

References

Bois, P., Lenfant, J. 1990. Isolated cells of the frog sinus venosus: properties of the inward current activated during hyperpolarization. *Pfluegers Arch.* **416**:339–346

Callewaert, G., Carmeliet, E., Vereecke, J. 1984. Single cardiac Purkinje cells: general electrophysiology and voltage-clamp analysis of the pace-maker current. *J. Physiol.* **348**:643–661

Chesnoy-Marchais, D. 1982. A Cl^- conductance activated by hyperpolarization in *Aplysia* neurones. *Nature* **299**:359–361

Chesnoy-Marchais, D. 1983. Characterization of a chloride conductance activated by hyperpolarization in *Aplysia* neurones. *J. Physiol.* **342**:277–308

Choi, M.S.K., Cooke, B.A. 1990. Evidence for two independent pathways in the stimulation of steroidogenesis by luteinizing hormone involving chloride channels and cyclic AMP. *FEBS Lett.* **261**:402–404

DiFrancesco, D. 1982. Block and activation of the pace-maker current in calf Purkinje fibres: effects of potassium, caesium and rubidium. *J. Physiol.* **329**:485–507

DiFrancesco, D. 1984. Characterization of the pace-maker current kinetics in calf Purkinje fibres *J. Physiol.* **348**:341–367

DiFrancesco, D. 1985. The cardiac hyperpolarizing-activated current, i_f. Origins and developments. *Prog. Biophys. Biol.* **46**:163–183

DiFrancesco, D., Ferroni, A., Mazzanti, M., Tromba, C. 1986.

Properties of the hyperpolarizing-activated current (i_f) in cells isolated from the rabbit sino-atrial node. *J. Physiol.* **377:**61–88

DiFrancesco D., Tortora, P. 1991. Direct activation of cardiac pacemaker channels by intracellular cyclic AMP. *Nature* **361:**145–147

Duchatelle, P., Joffre, M. 1987. Calcium-dependent chloride and potassium currents in rat Leydig cells. *FEBS Lett.* **217:**11–15

Duchatelle P., Joffre, M. 1990. Potassium and chloride conductances in rat Leydig cells. Effects of gonadotrophins and cyclic adenosine monophosphate *J. Physiol.* **428:**15–37

Dufau, M.L. 1988. Endocrine regulation and communicating functions of the Leydig cell. *Annu. Rev. Physiol.* **50:**483–508

Gögelein, H. 1988. Chloride channels in epithelia. *Biochim. Biophys. Acta* **947:**521–547

Hagiwara, N., Irisawa, H. 1989. Modulation by intracellular Ca^{2+} of the hyperpolarization-activated inward current in rabbit single sino-atrial node cells. *J. Physiol.* **409:**121–141

Joffre, M., Mollard, P., Régondaud, P., Gargouïl, Y.M. 1984. Electrophysiological study of single Leydig cells. II. Effects of ionic replacements, inhibitors and human chorionic gonadotrophin. *Pfluegers Arch.* **401:**246–253

Lotshaw, D.P., Levitan, I.B. 1987. Serotonin and forskolin modulation of a chloride conductance in cultured identified *Aplysia* neurons. *J. Neurophysiol.* **58:**922–939

Madison, D.V., Malesnka, R.C., Nicoll, R.A. 1986. Phorbol esters block a voltage-sensitive chloride current in hippocampal pyramidal cells. *Nature* **321:**694–697

Mager, R., Ferroni, S. Schubert, P. 1990. Adenosine modulates a voltage-dependent chloride conductance in cultured hippocampal neurons. *Brain Res.* **532:**58–62

Marty, A., Neher, E. 1983. Tight seal whole cell recording. *In:* Single-Channel Recording. B. Sakmann and E. Neher, editors; pp 107–122. Plenum, New York

Matthews, G., Neher, E., Penner, R. 1989. Chloride conductance activated by external agonists and internal messengers in rat peritoneal mast cells. *J. Physiol.* **418:**131–144

McCann, J.D., Li, M., Welsh, M.J. 1989. Identification and regulation of whole-cell chloride currents in airway epithelium. *J. Gen. Physiol.* **94:**1015–1035

Noulin, J.F., Joffre, M. 1992*a*. Cyclic AMP and calcium-activated chloride currents in Leydig cells isolated from mature rat testis. *Arch. Int. Physiol. Biochim. (in press)*

Noulin, J.F., Joffre, M. 1992*b*. Cyclic AMP dependence of the hyperpolarization-activated inward chloride current in Leydig cells isolated of rat testis. *Arch. Int. Physiol. Biochim.* **100(4):**A114 *(Abstr.)*

Parker, I., Miledi, R., 1988. A calcium-independent chloride current activated by hyperpolarization in *Xenopus* oocytes. *Proc. R. Soc. London B* **233:**191–199

Sharpe, R.M., Cooper, I. 1987. Relationship between the exposure of Leydig cells to factor(s) present in testicular interstitial fluid and changes in their capacity to secrete testosterone during culture or after hCG-induced desensitization. *Mol. Cell Endocrinol.* **51:**105–114

Singh, A.K., Afink, G.B., Venglarik, C.J., Wang, R., Bridges, R.J. 1991. Colonic Cl channel blockade by three classes of compounds. *Am. J. Physiol.* **260:**C51–C63

Solc, C.K., Wine, J.J. 1991. Swelling-induced and depolarization-induced Cl^- channels in normal and cystic fibrosis epithelial cells. *Am. J. Physiol.* **261:**C558–C674

Tsien, R.W. 1974. Effects of epinephrine on the pacemaker potassium current of cardiac Purkinje fibers. *J. Gen. Physiol.* **64:**293–318

Valverde, M.A., Mintenig, G.M., Sepúlveda, F.V. 1991. Cl^- conductance determines the membrane potential of unstimulated intestinal epithelial T84 cells. *Proc. Phys. Soc. J. Physiol.* **438:**334P

Van Ginneken, A.C.G., Giles, W. 1991. Voltage clamp measurements of the hyperpolarization activated inward current I_f in single cells from rabbit sino-atrial node. *J. Physiol.* **434:**57–83

Wine, J.J., Brayden, D.J., Hagiwara, G., Krouse, M.E., Law, T.C., Mueller, U.J., Solc, C.K., Ward, C.L., Widdicpmbe, J.H., Xia, Y. 1991. Cystic fibrosis, the CFTR, and the rectifying Cl channel. *In:* The Identification of the CF (Cystic Fibrosis Gene). Tsui et al., editors; pp. 253–272. Plenum, New York

Worrel, R.T., Butt, A.G., Cliff, W.H., Frizell, R.A. 1989. A volume-sensitive chloride conductance in human colonic cell-line T84. *Am. J. Physiol.* **256:**C1111–C1119

Received 25 June 1992; revised 14 October 1992